A Hidden Markov Model of the Breaststroke Swimming Temporal Phases Using Wearable Inertial Measurement Units

Farzin Dadashi[1], Arash Arami[1], Florent Crettenand[2], Gregoire P. Millet[2], John Komar[3], Ludovic Seifert[3], and Kamiar Aminian[1]

[1]Laboratory of Movement Analysis and Measurement, École Polytechnique Fédérale de Lausanne, Lausanne, Switzerland
[2]Institute of Sport Sciences, University of Lausanne, Lausanne, Switzerland
[3]CETAPS Laboratory, Sport Sciences Faculty, University of Rouen, Rouen, France
Email: farzin.dadashi@epfl.ch

***Abstract*— The recent advances in wearable inertial sensors opened a new horizon for pervasive measurement of human locomotion even in aquatic environment. In this paper we proposed an automatic approach of detecting the key temporal events of breaststroke swimming as a tentatively explored technique due to the complexity of the stroke. We used two inertial measurement units worn on the right arm and right leg of seven swimmers to capture the kinematics of the breaststroke. The detection of the temporal phases from the inertial signals was undertaken in the framework of a Hidden Markov Model (HMM). Supervised learning of the HMM parameters was achieved using the reference data from manual video analysis by an expert. The outputs of two well-known classifiers on the inertial signals were fused to unfold the input space of the HMM for an enhanced performance. An average correct phase detection of 93.5% for the arm stroke, 94.4% for the leg stroke and the minimum precision of 67 milliseconds in detection of the key events, suggests the accuracy of the method.**

Keywords- Hidden Markov Model; swimming; inertial measurement unit; feature extraction; linear classifier

I. INTRODUCTION

Sport technology developments target a broad spectrum of individuals from amateurs working on self-improvement programs to elite athletes in both on-land and in-water sports. A remarkable part of these developments belongs to monitoring tools where a physiological or spatiotemporal parameter can be measured during athlete's workouts [1]. By monitoring the temporal events of locomotion during the training or competition the technical differences between elite and recreational athletes can be investigated. Indeed, the analysis of these differences helps the coaches to design personal optimized plans for the trainees.

The breaststroke swimming is characterized by an alternative action of the arms and the legs followed by the limbs gliding phases and then the coinciding underwater recovery of the limbs. The arm-leg motor organization gives rise to the swimmer's speed fluctuations [2], and governs the breaststroke energy cost [3]. It has been shown that elite swimmers tend to diminish the discontinuity of the arm and leg actions for a sprint pace [3]. Specifically, a shorter glide time is observed in the higher speeds.

Considering the intricacies of measurement in water, the modalities that can be used for the study of locomotion in water are very limited. The visual inspection of the video footage by an expert has been usually used for the identification of the swimming temporal phases, though being time consuming. The video based system can provide quantitative information about the swimming technique along with the visual feedback [4]. Yet, the system focuses on one swimmer at a time and has a limited field of view that covers a few cycles of the swimming trial at each lap. This limited number of cycles cannot be a suitable representative of locomotion variability that is the principal interest in dynamical system framework of motor control and learning.

The deployment of the wearable inertial measurement units (IMU) is a new trend to extract the sport activity temporal phases automatically as previously reported in running [5], ski jumping [6] and baseball [7]. Ohgi et al. were the first ones who used a wrist-worn IMU sensor to characterize the stroke phases in breaststroke and front crawl swimming [8]. They did not provide any validation result on the accuracy of their method for the detection of temporal phases. Recently, a method to extract front crawl phases using a network of three body worn IMUs on the forearms and the sacrum has been proposed [9]. The general tendency for phase detection in previous works was to examine a single sensor channel for a signal peak or the time instant when the signal passes a threshold [10]. However, the phase transition results in a change in different modalities of a 3D inertial signal that cannot be necessarily captured in form of a signal peak or a single threshold. The supervised training of a pattern classifier can be a more effective approach to identify different phases of an activity [11].

In order to detect the temporal phases during the breaststroke, we used a Hidden Markov Model (HMM) as the framework to learn the kinematic signal patterns in different phases of the breaststroke cycle. We hypothesized that the different phases of the arm and leg movement during the breaststroke involve specific

statistical properties that can be used for the supervised learning of the HMM.

II. Data Collection Protocol

A. Subjects and Materials

Seven well-trained national level swimmers (4 males & 3 females, 17.4±1.8 yrs, 175.3±7.2 cm, 63.6±7.8 kg) participated in this study. The swimmers were equipped with two IMUs (Physilog®, BioAGM, CH), each IMU included a 3D accelerometer (±10g), a 3D gyroscope (±1200°/s) and an embedded data logger recording at 100Hz. One of the IMUs was placed on the dorsal side and distal end of the right forearm of the swimmer. The second IMU was positioned on the tibia just above the medial malleolus. The main assumption of our study was that there are common kinematics amongst swimmers that give rise to the detection of temporal phases using the IMUs on the forearm and the shank. Therefore, to be insensitive to the placement of the IMUs, a functional calibration procedure was performed to align the sensors' axes to the anatomical body axes as described in [6].

After a regular warm-up, each swimmer performed three 200-m trials in a 50-m indoor pool, at a constant submaximal intensity in breaststroke, with 5-min rests between trials. The intensity was 70% of breaststroke 200-m personal best time, for a target speed of 0.97m/s for males and 0.84m/s for females. This intensity was chosen to perform the analysis in a stable velocity. The swimmers were asked to maintain the planned speed by following the immerged stick of the operator walking along the pool deck with a distance <1 m.

The swimming trials were video-taped by two underwater cameras 0.6m below the water (Sony compact FCB-EX10L, f=50Hz). One camera filmed the swimmer from the frontal view, the other from the side view. The side view could capture 2 to 3 complete cycles at each 50m lap. Both cameras were connected to a timer, a video recorder and a screen to mix and genlock the frontal and side views on the same screen. A pushbutton, which started the IMUs' data acquisition, also provided a flashlight in front of the video cameras to synchronize the IMUs with the reference.

The protocol was approved by the ethical committee of university of Lausanne and followed the Declaration of Helsinki. The protocol was explained to the swimmers, who then gave their written consent.

B. The Reference Data: Video-based Extraction of the Breaststroke Temporal Phases

An expert extracted the breaststroke phases manually based on the description of the phases from the video sequences in the following paragraphs. We used this data as the reference data in our study.

A complete cycle of the arm and leg action during breaststroke can be divided into three main phases i.e. glide, propulsion and recovery. The definition of the phases using the video footage in our study is based on the work of Seifert et al. [2]. Fig. 1 illustrates these phases. The three main actions of the arm stroke are described as follows:

- Arm glide: corresponds to the time between the fully extended position of the arms and the beginning of the backward movement of the hands.
- Arm propulsion: this is the time between the beginning of the backward movement of the hands and the forward drive of the elbows.
- Arm recovery: corresponds to the time between the forward elbow drive to the next cycle's fully extended position of the arms.

The leg motor pattern during one cycle is divided into:

- Leg propulsion: corresponds to the time between the beginning of the backward movement of the shanks – with the knee joint being maximally flexed – and the leg extension.
- Leg glide: this is the time between the beginning of the leg extension and beginning of the knee flexion (determined by lifting of the heels).
- Leg recovery: this is the time between the beginning of the knee flexion and the next cycle's backward movement of the shanks.

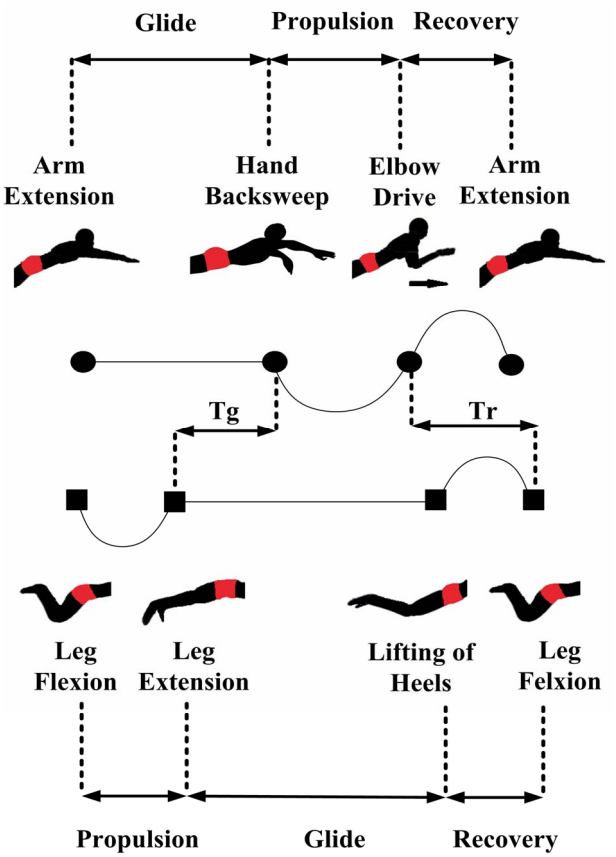

Figure 1. Illustration of the arm and leg stroke phases in the breaststroke. The key events that determine the beginning and the end of each phase are also presented.

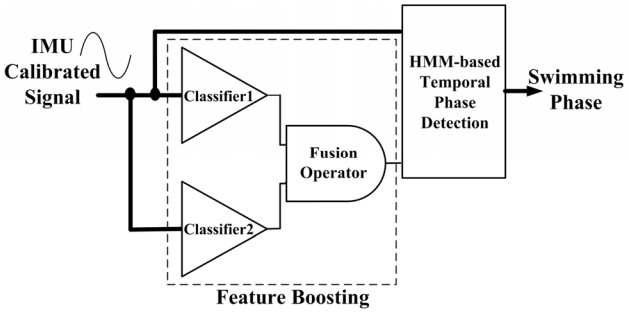

Figure 2. Feature boosting process for enhancing the performance of HMM-based phase detection algorithm

The glide time, *Tg*, between legs and arms propulsion starts from the end of leg propulsion until the start of the hands backsweep. The time gap, *Tr*, denotes the time when one of the limbs (arms or legs) starts its recovery and the time when both arms and legs finish their respective recoveries. According to Seifert et al. [2], a glide pattern occurs for a negative *Tg*, continuous pattern is for *Tg=0*, and overlapped pattern is for a positive *Tg* that indicates an overlap between the propulsion of the arms and legs. The time gap between propulsive action of legs and arms shows the propulsive discontinuity that is called total time gap (TTG) and can be calculated as the sum of *Tg* and *Tr*.

III. Detection of the Breaststroke Phases Based on a Hidden Markov Model (HMM)

The IMUs data were used as the observation in an HMM to automatically detect the stroke phases of the arm and leg movement. Yet, before training the HMM, we augment its input feature space by a feature boosting process where a supervised training of different classifiers is performed to learn the stroke phases. The output of these classifiers is then fused to form a new feature vector along with the IMU reading. This new feature space is easier to be learnt by HMM and results in improved phase detection. Fig. 2 depicts a block diagram of this procedure.

A. HMM Implementation for Breaststroke Phase Detection

The biomechanical constraint of breaststroke implies that it is not possible to go from one phase to another without passing through an intermediate phase. For example based on the phase definition in section II.B, after arm propulsion the arm recovery takes place before gliding with fully extended arms. Such a constraint can be efficiently modeled using so-called left-right cyclic HMM.

As illustrated in Fig. 3 only transition to the next phase or self-transitions are allowed in a left-right cyclic HMM. Mathematically speaking, the phase detection problem using a HMM is equivalent to finding the most probable sequence of states $\{S_i\}_{i=t_0}^{t_0+n}$ (for some $t_0, n \in \mathbb{N}$ and $S_i \in \{1,2,3\}$ corresponding to the three phases recovery, glide and propulsion respectively) providing that we have the observations $\{\vec{X}_i\}_{i=t_0}^{t_0+n}$ where $\vec{X}_i$ consists of the IMU readings and the features augmented by the feature boosting process. By assuming that the next state just depends on the state at the present time (Markov property), the problem of finding the most probable state sequence, S^*, can be presented as:

$$\begin{aligned} S^* &= \underset{S}{\operatorname{argmax}}\ p\left(\{S_i\}_{i=t_0}^{t_0+n} \middle| \{\vec{X}_i\}_{i=t_0}^{t_0+n}\right) \\ &= \underset{S}{\operatorname{argmax}}\ p\left(\{S_i\}_{i=t_0}^{t_0+n}, \{\vec{X}_i\}_{i=t_0}^{t_0+n}\right) \\ &= \underset{S}{\operatorname{argmax}}\ p(S_{t_0}) p(\vec{X}_{t_0}|S_{t_0}) \prod_{i=t_0+1}^{t_0+n} p(S_i|S_{i-1}) p(\vec{X}_i|S_i) \end{aligned} \quad (1)$$

where S^* can be computed by the Viterbi algorithm [12] providing that all the elements in (1) are known. The first element in the right hand side of (1), $p(S_{t_0} = i)$, with $i = 1,2,3$ is initial probability of the states that can be calculated as the frequency of the states in the training data. The second element forms the state transition probability matrix, A:

$$A_{ij} = p(S_t = i|S_{t-1} = j),\ \ \sum_i A_{ij} = 1 \quad (2)$$

where $i, j = 1,2,3$. A_{ij} can be calculated as the number of samples in the training set with a transition from state i to state j divided by the total number of samples labeled as state j. The last term in (1) denotes the emissions from each state that can be observed (measured) as the sensor readings along with the augmented features. The emissions at each state were modeled as multivariate Gaussian mixtures (MGM). The number of modalities in the MGM was determined by examining the histogram of the IMU data for each state. The labeled video footage (synchronized with the sensors) was used as the reference

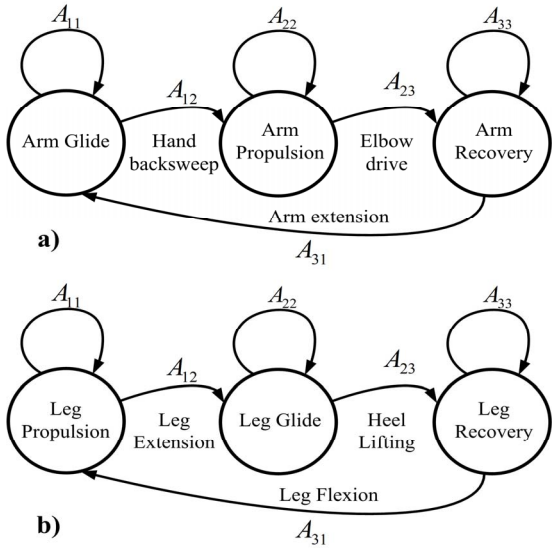

Figure 3. Left-right state transition of the HMM for the arms stroke (panel a) and the legs stroke (panel b). Each state of HMM is presented by a circled label and possible state transitions are shown by arrows and corrseponding probability is shown by A_{ij}. The labels on arrows identify the key movement that initiates the next state.

to label the IMU data. This labeled IMU data was then used to train the HMM parameters in (1). The Viterbi decoding of the observations in left-right HMM turns out to be prone to erroneous events that consisted of missing an event or invalid detection of an event when the transition did not take place (*deletion* and *insertion*, respectively). By rejecting the transitions where the duration of the new state is less than a predefined minimum phase length, this problem can be remedied [13]. We selected the minimum acceptable phase length to be 80ms.

B. Feature Boosting with Classifier Fusion

The main idea of the feature boosting scheme was to learn the boundaries of the three phases of breaststroke data by two classifiers. Each classifier could learn parts of the feature space more accurately than the other. Therefore, we fused these two classifiers for more accurate labeling of the feature data. The original feature space was constructed using 6D IMU measurements. The result of the fusion of the classifiers was appended to the original feature space to build the boosted feature space. The following paragraphs explain this procedure.

Let $\chi_{train} = \{\vec{x}_i\}_{i=1}^{N} \subset \mathbb{R}^6$ be the training feature space constructed from 6D IMU measurements and $\{y_i\}_{i=1}^{N}$ be the corresponding class labels where $y_i \in \{1,2,3\}$. We defined the first classifier g as a quadratic projection from feature space χ_{train} into the class label space ψ i.e. $g: \chi_{train} \rightarrow \psi$, where $\psi = \{1,2,3\}$ corresponds to the three classes recovery, glide and propulsion respectively. We defined $g(.)$ as:

$$g(\vec{x}_i) = \underset{k}{\operatorname{argmax}} \left({\vec{x}_i}^t Q_k \vec{x}_i + L_k \vec{x}_i + b_k \right) \quad (3)$$

where $k = 1,2,3$ and $Q_k \in \mathbb{R}^6 \times \mathbb{R}^6$, $L_k \in \mathbb{R}^6$, $b_k \in \mathbb{R}$. The set of parameters $\Omega_k = \{Q_k, L_k, b_k\}$ define the boundary between class k and other classes [14]. Consequently, the posterior probability for class k for the given $\vec{x}_i$ and the model g can be calculated by (4):

$$p(\psi = k|\vec{x}_i, g) = \frac{exp({\vec{x}_i}^t Q_k \vec{x}_i + L_k \vec{x}_i + b_k)}{\sum_{j=1}^{3} exp({\vec{x}_i}^t Q_j \vec{x}_i + L_j \vec{x}_i + b_j)} \quad (4)$$

The second classifier was a nonparametric probability density estimator with a Gaussian smoothing kernel, $K_h(.)$ where h shows the bandwidth of the kernel. The posterior probability for class k for the given $\vec{x}_i$ and the kernel K_h is given by:

$$p(\psi = k|\vec{x}_i, K_h) = \frac{\sum_{\vec{x} \in K_h} K_h(\vec{x}_i - \vec{x})\ I_k(y)}{\sum_{\vec{x} \in K_h} K_h(\vec{x}_i - \vec{x})} \quad (5)$$

where $I_k(y) = 1$ if $y = k$ and otherwise $I_k(y) = 0$ [15]. The bandwidth parameter was learnt by varying h from zero to one by steps of 0.01 on the normalized feature space and then taking the h value that led to the maximum correct classification ratio on the training set.

Now let $p(\psi = k|\vec{x}_i, classifier)$ show the probability that *classifier* assigns the class label k to the input $\vec{x}_i$. We used the ordered weighted averaging (OWA) to fuse the information from the two classifiers [16]. To this end, for each class label we sorted $p(\psi = k|\vec{x}_i, classifier)$ in a descending order so that:

$$\begin{aligned} {a_1}^k &= max\{p(\psi = k|\vec{x}_i, g(\vec{x}_i)), p(\psi = k|\vec{x}_i, K_h(\vec{x}_i))\} \\ {a_2}^k &= min\{p(\psi = k|\vec{x}_i, g(\vec{x}_i)), p(\psi = k|\vec{x}_i, K_h(\vec{x}_i))\} \end{aligned} \quad (6)$$

The total preference for the class label k, $\Theta({\vec{x}_i}^k)$ was then calculated as:

$$\Theta\left({\vec{x}_i}^k\right) = \lambda {a_1}^k + (1 - \lambda) {a_2}^k \quad (7)$$

where the parameter $\lambda \in [0.5,1]$ determines the degree of preference of the classifier with higher confidence. To find λ for the leg IMU and the forearm IMU separately, we varied it from 0.5 to one with 0.01 steps size for which the maximum correct classification ratio on the training dataset was obtained. The vector $\Theta({\vec{x}_i}^k)$ was augmented to the original IMU signals as the input of HMM.

C. Statistical Evaluation of the Algorithm

The abovementioned algorithm was applied to the forearm and shank IMU signals separately. The leave-one-out cross validation was conducted to evaluate the algorithm performance on different test sets. Indeed, we trained the HMM using the data from all subjects but one and then the data from the remaining subject was used to test the proposed method. This procedure was performed for all the athletes one by one.

To assess the performance of our algorithm in the detection of temporal events, the key events (explained in section II.B) were estimated by the proposed method as the transition instants between the phases and then TTG was also calculated. The accuracy and precision (Mean and SD) were calculated as the difference of the reference phase detection (video labeling) and the values estimated by our algorithm. The median absolute deviation (MAD) of the differences was also calculated as a measure of dispersion. A repeated measure ANOVA was performed to verify the effect of trials and athletes on the difference between IMU-based phase detection and the reference.

In order to evaluate how accurately the different phases can be labeled, we calculated the sensitivity and the specificity of the phase detection algorithm. Sensitivity is calculated as the percentage of correctly labeled instances with the algorithm whereas specificity shows the percentage of instances that genuinely does not belong to a phase and predicted as not belonging to that phase.

IV. Results

A total number of N = 168 video cycles was captured and labeled by the expert. The λ value of the OWA algorithm in feature boosting for the leg IMU turned out to be 0.77

and for the forearm IMU equal to 0.82. Fig.4 presents a typical result of the phase detection algorithm on the forearm IMU compared to the reference labeling by the expert. After applying the minimum phase duration condition on the decoding result of the Viterbi algorithm, no instances of deletion and insertion were observed.

Table I reports the difference between the two systems in the detection of the key temporal instants and estimation of TTG. The biggest error variability happens for the arm extension that is equivalent to 2.9 video frames. The error variability for TTG was in order of 3.1 video frames. It is noteworthy that the accuracy and precision of the estimation of *Tg* is -11±52ms. Repeated measures ANOVA showed that the difference between our method and the reference is not influenced by either of athlete or trial factors ($p > 0.1$).

Table II represents the sensitivity and specificity of the phase detection algorithm for the arm and leg strokes. The lowest average correct classification ratio (sensitivity) is for the arm recovery phase that is 90.8%.

Fig. 5 shows the average sensitivity of the phase detection as a result of: 1) classification process that we used for feature boosting, 2) the right-left HMM without feature boosting and finally 3) the ensemble of these two

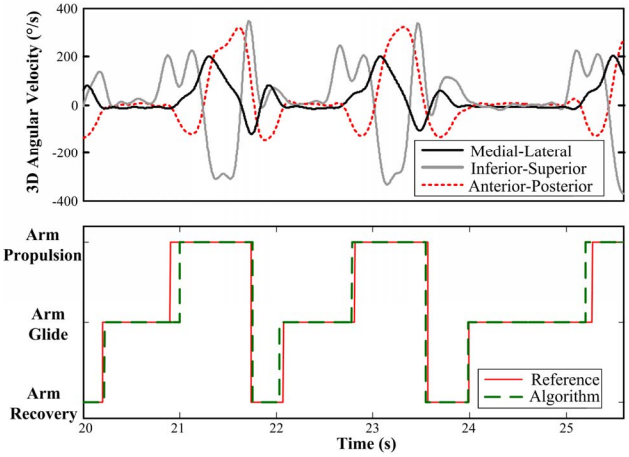

Figure 4. A typical result of HMM phase detection on the forearm IMU signal compared to the reference. For the sake of clarity, only the 3 channels of the gyroscope are shown (see [17] for the definition of axes)

TABLE I. TIMING ERROR (VIDEO - IMU) OF THE ARM AND LEG STROKE (MEAN AND SD) AND ERROR VARIABILITY (MAD) ALL IN MILLISECONDS.

	Error Mean	*Error SD*	*Error MAD*
Hand Backsweep	25	47	31
Elbow Drive	-4	30	22
Arm Extension	9	67	58
Leg Flexion	7	31	21
Leg Extension	13	58	53
Lifting of Heels	-11	43	29
TTG	-20	76	61

TABLE II. AVERAGE PERFORMANCE OF THE BOOSTED HMM IN PHASE DETECTION

	Arm Phase Detection	*Leg Phase Detection*
Sensitivity	93.5%	94.4%
Specificity	96.2%	97.2%

steps. The sensitivity of the arm phase detection in the feature boosting process was 90.7% and for the HMM was 87.3%. For the leg phase detection, the feature boosting process showed a sensitivity of 89.8% and the HMM sensitivity was 88.4%.

V. DISCUSSION

The result of our study validates that by using two wearable IMUs on the forearm and the leg, the main temporal phases of the breaststroke swimming can be reliably detected. The systematic error (accuracy) of our method on detection of the key events of arm-leg stroke is always less than 25ms that is approximately equivalent to one video frame i.e. resolution of the video analysis. The precise estimation of leg extension time and backsweep of the hands, leads to a precise estimation of *Tg* as the core metric of coordination in the breaststroke [18]. The ANOVA result confirmed that the performance of the algorithm is not swimmer dependent.

As for the timing error of the key events, the arm extension and the leg extension showed the biggest estimation error as presented by MAD values. Two main sources are conceivable for this error. Firstly, the error can be originated from the high variability in the range of motion and range of angular velocity when the swimmers extend their legs during the propulsive phase of leg and extend their arms during the arm recovery. This variability can be more complicated for the HMM to learn considering the size of the dataset. Yet, the second source of error can be in the variability of the labeling of the phases since the detection of a fully extended limb by visual inspection can be prone to subjective error. Besides,

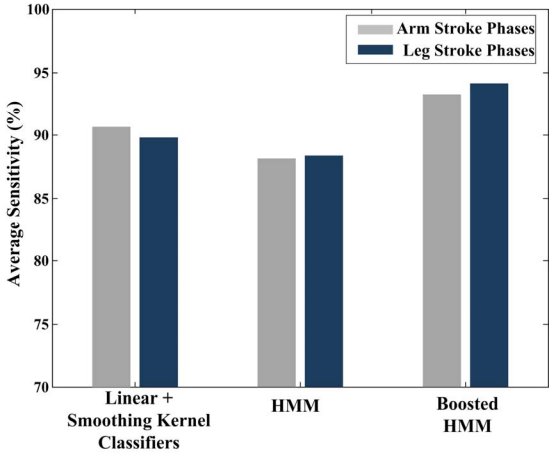

Figure 5. The effect of input feature boosting on the performance of HMM-based phase detection algorithm

vertical inclination of the trunk during the breathing movement is a tricky phase that can be confounded with beginning of the leg flexion during video analysis. In other words, although the identification of the temporal phases obtained by visual scrutiny of the video from the expert is considered as the "standard" method of the temporal phase detection in swimming, the manual video analysis is not a true gold standard, as it can have the same order of error as the algorithm proposed in the present study.

The left-right HMM probabilistic framework allowed us to impose the ordinal occurrence of the phases -as a constraint of the swimming locomotion- in our algorithm. Furthermore, the feature boosting scheme that we used to enrich the input space of the HMM, improved the result of the phase detection algorithm meaningfully. It can clearly be seen in Fig. 5 that our method outperforms the either of the two separate algorithms. The TTG estimation error MAD reduces from 5.4 frames in single HMM scheme to 3.1 frames in the boosted HMM framework. It should be mentioned that the supervised HMM parameter learning process was used in this work that simplifies the parameter estimation in the lack of large data sets [19].

By deploying the wearable IMUs in the proposed phase detection algorithm, we provided a tool to address the inter-cyclic variability assessment that is not a viable option using video based systems with a field of view restricted to 2 to 3 cycles. The estimation of the inter-cyclic variability is of utmost interest for the coaches to design pacing strategies and for the sport scientists to study the changes that occur in the metabolic response due to the variability of movement.

VI. Conclusion and Future Work

In this paper, we proposed a new method of estimating the breaststroke temporal phases automatically by means of two wearable IMUs that provided promising results. Our method contrary to the manual video processing, estimates the temporal features in a timely manner and does not require any cumbersome equipment installation in the swimming pool. The proposed way of boosting the input space of the HMM-based classifier, resulted in enhanced performance in the phase detection.

The use of IMUs in different configurations, as proposed in this paper and our previous works [9, 20] offers a new potential to pinpoint the technical weaknesses of the athletes in different swimming styles. The extension of the work will be focused on the validation of the system on the recreational swimmers that presumably show more variability in their swimming technique.

Acknowledgment

This work was supported by the Swiss National Science Foundation (SNSF) (grant no. 320030-127554). The work was also partly financed by the Interinstitutional Centre of Translational Biomechanics (CBT).

References

[1] P. Bonato, "Wearable sensors and systems," *IEEE Engineering in Medicine and Biology Magazine,* vol. 29, pp. 25-36, 2010.

[2] L. Seifert and D. Chollet, "A new index of flat breaststroke propulsion: A comparison of elite men and women," *Journal of Sports Sciences,* vol. 23, pp. 309-320, 2005.

[3] J. Vilas-Boas, R. Fernandes, and T. Barbosa, "Intra-cycle velocity variations, swimming economy, performance and training in swimming," *World Book of Swimming: From Science to Performance,* pp. 119-134, 2010.

[4] A. J. Callaway, J. E. Cobb, and I. Jones, "A comparison of video and accelerometer based approaches applied to performance monitoring in swimming," *International Journal of Sports Science and Coaching,* vol. 4, pp. 139-153, 2009.

[5] E. Bergamini, et al., "Estimation of temporal parameters during sprint running using a trunk-mounted inertial measurement unit," *Journal of Biomechanics,* vol. 45, pp. 1123-1126, 2012.

[6] J. Chardonnens, J. Favre, B. Le Callennec, F. Cuendet, G. Gremion, and K. Aminian, "Automatic measurement of key ski jumping phases and temporal events with a wearable system," *Journal of sports sciences,* vol. 30, pp. 53-61, 2012.

[7] H. Ghasemzadeh and R. Jafari, "Coordination analysis of human movements with body sensor networks: A signal processing model to evaluate baseball swings," *IEEE Sensors Journal,* vol. 11, pp. 603-610, 2011.

[8] Y. Ohgi, H. Ichikawa, and C. Miyaji, "Microcomputer-based acceleration sensor device for swimming stroke monitoring," *JSME International Journal, Series C: Mechanical Systems, Machine Elements and Manufacturing,* vol. 45, pp. 960-966, 2002.

[9] F. Dadashi, F. Crettenand, G. Millet, L. Seifert, J. Komar, and K. Aminian, "Frontcrawl propulsive phase detection using inertial sensors," in *29 International Conference on Biomechanics in Sports* 2011, pp. 855-858.

[10] B. Mariani, H. Rouhani, X. Crevoisier, and K. Aminian, "Quantitative estimation of foot-flat and stance phase of gait using foot-worn inertial sensors," *Gait and Posture,* 2012.

[11] E. Guenterberg, H. Ghasemzadeh, and R. Jafari, "A distributed hidden markov model for fine-grained annotation in body sensor networks," in *Wearable and Implantable Body Sensor Networks (BSN)*, 2009, pp. 339-344.

[12] L. R. Rabiner, "Tutorial on hidden Markov models and selected applications in speech recognition," *Proceedings of the IEEE,* vol. 77, pp. 257-286, 1989.

[13] A. Mannini and A. M. Sabatini, "Gait phase detection and discrimination between walking-jogging activities using hidden Markov models applied to foot motion data from a gyroscope," *Gait and Posture,* vol. 36, pp. 657-661, 2012.

[14] D. M. J. Tax and R. P. W. Duin, "Using two-class classifiers for multiclass classification," in *International Conference on Pattern Recognition*, 2002, pp. 124-127.

[15] K. Hechenbichler and K. Schliep, "Weighted k-nearest-neighbor techniques and ordinal classification," *discussion paper 399, SFB 386 der Ludwig-Maximilians-Universität München,* p. 16, 2004.

[16] R. R. Yager, "On ordered weighted averaging aggregation operators in multicriteria decisionmaking," *IEEE Transactions on Systems, Man and Cybernetics,* vol. 18, pp. 183-190, 1988.

[17] G. Wu, et al., "ISB recommendation on definitions of joint coordinate systems of various joints for the reporting of human joint motion - Part II: Shoulder, elbow, wrist and hand," *Journal of Biomechanics,* vol. 38, pp. 981-992, 2005.

[18] D. Chollet, L. Seifert, H. Leblanc, L. Boulesteix, and M. Carter, "Evaluation of arm-leg coordination in flat breaststroke," *International Journal of Sports Medicine,* vol. 25, pp. 486-495, 2004.

[19] L. R. Welch, "Hidden Markov models and the Baum-Welch algorithm," *IEEE Information Theory Society Newsletter,* vol. 53, pp. 1-14, 2003.

[20] F. Dadashi, F. Crettenand, G. P. Millet, and K. Aminian, "Front-Crawl Instantaneous Velocity Estimation Using a Wearable Inertial Measurement Unit," *Sensors,* vol. 12, pp. 12927-12939, 2012.